Stereoselective peptide synthesis in alkaline hydrothermal vent conditions

Daniel P. Molland[1,*], Isabella B. Rhyu[1], Jon Wade[2,*], Jason R. Schnell[1,*]

[1.]Department of Biochemistry, University of Oxford, South Parks Road, OX1 3QU

[2.]Department of Earth Sciences, University of Oxford, South Parks Road, OX1 3AN, UK

***Corresponding Authors:** Daniel P. Molland, Jon Wade, and Jason R. Schnell

Keywords: origin of life, abiogenesis, peptide synthesis, cysteine

Abstract

Modern proteins are composed exclusively of L-amino acids but the origin of L-stereospecificity is unresolved. Carbonaceous meteorites were a significant source of organic matter on early Earth and commonly contain ten proteogenic amino acids in racemic mixtures. In conditions relevant to early Earth hydrothermal vents, surface-catalyzed peptide syntheses of these proteogenic mixtures show modest reaction rates and no significant stereoselectivity. However, we show that the presence of cysteine significantly increases peptide synthesis yields in the presence of silicate surfaces, with synthetic yields displaying a strong stereoselective bias towards L-cysteine. In a hydrothermal vent solvent model, L-cysteine doubles the increase in peptide synthetic yields compared to D-cysteine, as indicated by UV absorption, NMR, and mass spectrometry. Solid state NMR confirms that cysteine associates with silicates at alkaline pH via both carboxylate and sulfur groups. This adsorption results in a stereospecific orientation of the reactive amino group for surface-adsorbed bivalently charged amino acids detectable by Polarization-Resolved IRRAS. This stereospecific amino group reorientation provides a novel mechanism for abiotic peptide synthesis favoring L-amino acids on achiral surfaces, which is applicable to any bivalently charged amino acid at alkaline pH. Our findings here, that cysteine is incorporated stereoselectively in surface-catalyzed peptide synthesis, combined with the metal-binding capability of abiotically synthesized cysteine-bearing peptides, emphasizes the potential benefits of amino acids with sulfur functional groups to fundamental processes in early life and the potential usefulness of such amino acids as biosignatures.

Introduction

Proteins are essential components of life, but their pre-biotic origins remain unresolved (1). Carbon-rich meteorites contain up to 2300ppm of amino acids and are proposed to have been a major source of the early Earth's inventory of organic molecules (2,3) Amino acids and their peptide polymers may have formed alongside, or even before, the first RNAs in a "peptide-RNA world"(4).

The amino acids glycine, alanine, aspartate, glutamate, valine, isoleucine, leucine, serine, threonine, and proline, are found in carbonaceous meteorites and together are known as the abiotic amino acid set (5, 6) This set is restricted to neutral or negatively charged sidechains and offers limited potential functionality and no known mechanism for facilitating protein-mediated redox activity due to their low sidechain nucleophilicity (7).

Several mechanisms have been proposed for synthesis of peptides from this set, including salt induced peptide formation(8) and activating agent catalyzed peptide synthesis (9, 10). The best explored of these synthetic routes is surface-catalyzed peptide synthesis, first proposed by Bernal *et al.* (11) and since documented under a wide range of reaction conditions (12) and minerals.(13) Mineral surfaces catalyze peptide synthesis by binding amino acids, typically through electrostatic interactions, and increasing local amino acid concentrations (12, 13) The extent to which a particular surface can enhance peptide synthesis is driven predominantly by residence times on the mineral surface, which depend on the strength of the interaction and electrostatics that affect diffusion near the surface (13).

Abiotic peptide synthesis is facilitated by deprotonation of the zwitterionic amino group to form the more nucleophilic NH_2 group, which occurs at alkaline pH (~9.52) (14). Moderate heating also facilitates synthesis since peptide bond formation is favorable at >60˚C,(15)(16) but diketopiperazine formation is favored at ≥120˚C (17). This observation has led to the proposal of alkaline hydrothermal vent systems, such as the white smokers of the Atlantis Massif, as possible sites for the formation of Earth's first proteins (18). The Enceladian ocean is proposed to contain similar vents (19), providing hot (~90˚C), alkaline (pH ~9.5) conditions (20,21).

While peptide synthesis from amino acids can be catalyzed by high salt, metals, and surfaces, peptide bond yields are typically low and peptide lengths typically limited to ~2-6 amino acids (22, 18, 23, 24, 25). In surface-catalyzed peptide synthesis, this limitation is a consequence of the relatively weak association between peptides and the mineral surface, and the formation of peptide-chain terminating end products such as piperazines (22). In addition, stereoselectivity in abiotic peptide syntheses, which may have contributed to the L-amino acid homochirality observed in life today (26), is typically low or absent. A <10% preference for L-amino acids was observed for metal-mediated catalysis in high salt conditions but the mechanism not identified (27), and reported peptide syntheses with >25% stereoselectivity depend on chiral templating minerals (28) or chiral biotic precursors (29). Thus, none of the currently described synthetic processes provide a general mechanism for high yield and stereoselective synthesis of longer peptides (18).

We hypothesize that the addition of amino acids with higher reactivity to a surface-catalyzed peptide synthesis system could circumvent both low peptide yields and the low

stereoselectivity of previously reported approaches. While excluded from previous surface-catalyzed peptide synthesis studies, the sulfur functional group of cysteine is dramatically more nucleophilic than any other amino acid (7) and anticipated to greatly increase surface interactions of cysteine monomers and cysteine-bearing peptides in surface/solvent interfaces. All biogenic proteins have methionine as the first amino acid, suggesting sulfur-bearing amino acids may have been present in the earliest stages of life, and previous work suggests that the presence of sulfur was essential to the origin of life's metabolic pathways (30) and of peptide ligation in aqueous solutions(31, 32), but the effects of including a sulfur-bearing amino acid like cysteine in abiotic surface-catalyzed peptide synthesis systems has not yet been investigated.

Investigating abiotic peptide synthesis in the presence of simple amino acids with sulfur functional groups like cysteine is also motivated by the unique capabilities such amino acids could have provided to nascent life by generating peptides able to coordinate, and therefore utilize, soluble metal ions. Modern proteins often coordinate metabolically active transition metals such as iron, copper, nickel and cobalt through cysteine. The cysteine thiol can readily coordinate metals in solution (33), and in proteins like thioredoxins they directly mediate reduction-oxidation chemistry (34).

Here, we investigated the potential role of the highly nucleophilic thiol in abiotic peptide synthesis in a surface-based reaction mechanism. We found that the addition of cysteine in the presence of a silicate surface increased peptide synthesis 7.8-fold, producing peptides as large as 12 amino acids in length, and that peptide yields were 50% stereoselective for L-cysteine, over D-cysteine. Our results are consistent with an unusually strong stereospecific silicate mineral association mechanism for cysteine. We show that cysteine adsorbs onto the abundant mineral surface SiO_2 through both the carboxylate and sulfur groups simultaneously and that the amino group is stereospecifically oriented in the surface-bound state. We propose that the stereospecific surface orientation of the amino group in bivalently surface-bound L-enantiomers is responsible for the observed rate enhancement. Our work points to the possibility that the most efficient mechanism for stereoselective peptide bond formation is bivalent surface catalysis under alkaline reducing conditions like those found at hydrothermal vents. The increased abiotic yield and metal binding capability (35, 36) of thiols indicate that cysteine or other amino acids with sulfur functional groups could be essential ingredients for abiogenesis.

Results

Increased peptide synthesis yields and stereoselectivity with cysteine.

A reaction scheme was established based on the oxide mineral and amino acid reaction systems of Takahagi (17). All reaction mixtures contained a racemic meteoric amino acid mixture (MAAM) supplemented with an additional L- or D-amino acid at excess concentration to test its effect on peptide yields. The mineral surface was simulated with heat-sterilized pyroxene or fumed spectroscopy grade SiO_2 in borosilicate or polypropylene reaction vessels, and reaction mixtures were heated in reducing conditions at 90°C for the times indicated. Consistent with surface-catalysis, reactions in borosilicate vessels led to 1.8-fold increases in peptide yields over reactions in polypropylene vessels due to the additional silicate surface area (**Figure S1a**).

Initial assessment of peptide yield was conducted by UV-spectrophotometry.(37) Statistical significance of differences in absorption was determined through one way ANOVA with Tukey post hoc analysis to determine the effect of e ach tested excess amino acid on peptide yield compared to an L-alanine negative control (**Table S1**). In borosilicate reaction vessels, absorption of 230nm light (A_{230}) increased significantly after 48 hours in the presence of L-cysteine compared to reactions with either L-alanine (p=<0.0001) or D-cysteine (p=0.0006). In contrast, synthesis with excess L- or D-alanine (p=0.7172), and L-alanine or L-methionine (p=0.7021) did not result in significantly increased peptide yields, indicating that these enantiomers adsorbed to silicates similarly at alkaline pH. When compared to the mean absorbances for L-alanine, D-alanine and L-methionine, the presence of L-cysteine increased peptide bond yield 7.8-fold (±0.6), and D-cysteine increased absorbance 3.9-fold (±0.6) (**Figure 1a)**.

The presence of silicate surfaces significantly amplifies the catalytic effect of cysteine on peptide bond formation. In the absence of a silicate surface, peptide bond yields were increased approximately 3-fold, consistent with a previous report (31), and the addition of a silicate surface (pyroxene) increased this value another 6-fold (p=0.0015; two-tailed unpaired t-test) (**Figure 1b, Table S2**). The apparent rates of reaction after 48 hours for systems containing pyroxene and either L-cysteine, D-cysteine or L-alanine in 5mM excess were 0.76, 0.38, and 0.12 mM of peptide bonds per hour, respectively.

The depletion of monomeric amino acids and the formation of peptide species during the reaction was confirmed using solution NMR. Quantitative NMR (qNMR) measurements after 48-hour reactions with either L-cysteine or L-alanine indicated that 7.7-fold more monomeric L-cysteine was removed than L-alanine (**Figure 1c**). ^{1}H-^{1}H total correlation spectroscopy (TOCSY) of the reacted mixtures revealed signals consistent with cysteine $^{1}H_N$-$^{1}H_\alpha$ and $^{1}H_N$-$^{1}H_\beta$ correlations that were not observed in the unreacted control samples (**Figure 1e**).

Peptides synthesized with cysteine are compositionally diverse.

The synthesis products were further characterized by repeating the reactions using isotopically labelled amino acids for analysis by ^{13}C NMR spectroscopy. NMR spectra of products formed in the presence of $^{13}C_\beta$ L-cysteine after heating at 90°C for 48 hours indicated a large number of unique signals in the chemical shift range expected for non-oxidized cysteine $^{1}H_\beta$-$^{13}C_\beta$ and $^{1}H_\alpha$-$^{13}C_\alpha$ correlations, as well as amide ^{1}H to $^{1}H_\alpha$ and $^{1}H_\beta$, which were consistent with the formation of a diverse set of cysteine-bearing peptides (**Figure 2a-b**). In contrast to the reactions with cysteine, few unique signals were observed when synthesis was conducted in the presence of ^{13}C-labelled L-methionine (**Figure S3**).

Peptide compositions and lengths were evaluated using Trapped Ion Mobility Spectrometry Time-of-Flight (TIMS-TOF) mass spectrometry (MS) after 42 days at 90˚C followed by purification using C18 solid phase extraction (SPE). Synthesis conducted in the presence of L-cysteine generated the largest number of unique peptide detections (**Figure 2d**). The peptide diversities detected by TIMS-TOF MS were likely underestimated due to the C18 peptide purification conducted prior to HPLC/TIMS-TOF MS, which enriches samples in hydrophobic peptides (**Figure S4**). In the presence of L-cysteine, significantly larger numbers of unique peptides longer than four amino acids were detected compared to L-alanine (Mann Whitney Test, p=0.0188, **Table S3**), and peptides containing up to 12 amino acids were observed. In the presence of L-alanine the largest observed peptide was an 8-mer, and fewer unique peptides

were observed overall. Increases in the number of detectable peptides were also observed with D-cysteine compared to L-alanine, but not to statistical significance (p=0.1563) (**Figure S5**, **Table S4**). The increased detections of peptides in reactions with L-cysteine compared with D-cysteine and L-alanine were consistent with the yields determined from A_{230} and qNMR and supported a stereoselective bias toward L-cysteine.

Increased peptide yields with cysteine are due to the thiol.

The increased peptide yields with L- and D-cysteine compared to L-alanine correlate with the high nucleophilicity of the sidechain thiol, (7) which results in strong attachment to mineral surfaces. Reactions in the presence of L-homocysteine showed a comparable level of peptide bond formation to L-cysteine (**Figure S1b**) whereas L-methionine showed no statistically significant increase in peptide bond formation compared to L-alanine (**Figure 1b**). Reaction yields with excess L-aspartate were higher than the yields with excess L-alanine (**Figure S1b**), suggesting that attachment through the carboxylate sidechain can also contribute to increased yields. However, the yields with L-aspartate were much lower than that of reactions with excess L-cysteine, consistent with the much lower nucleophilicity (7) and weaker silicate binding of the sidechain carboxylate group (38).

We also observed a high correlation between peptide yield in the presence of different metal oxides and the corresponding metal-sulfur bond dissociation energies, confirming that the strength of attachment via the sulfur group to the mineral surface is the dominant factor affecting peptide yield (**Figure S3**). In contrast, silicate-sulfur bonds have very high dissociation energies and the yield in the presence of silicate was lower than expected from the trend observed for metal oxides, which may indicate that adsorption was no longer rate-limiting (39).

NMR and MS results supported the observations by UV spectroscopy that cysteine stereoselectively enhances peptide yield when in the presence of an oxide mineral surface. The stereoselective bias toward L-cysteine persisted at the lowest concentrations of amino acids tested (55µM) (**Figure 1d**), indicating that peptides generated abiotically in the presence of racemic cysteine monomers would be enriched with L-cysteine at a ratio similar to that of the observed peptide yield increase.

Cysteine silicate bivalent adsorption at alkaline pH

Based on the observed effects of the sidechain thiol on peptide yields, and that amino acids in neutral or alkaline pH can attach to mineral surfaces via charged groups (13, 38), we hypothesized that bivalent surface attachment to mineral surfaces via both the carboxylate and sulfur groups, concurrent with deprotonation of the amino group at alkaline pH, could provide a mechanism for the observed stereoselective differences in peptide yields. Two-point attachment of cysteine via its carboxylate and sulfur groups restricts rotation of the amino acid at the mineral surface, leading to stereospecific differences in the orientation of the amino group, which could affect either the energetics of surface attachment (e.g., through steric clash) or the rates of peptide bond formation through positioning of the amino group for nucleophilic attack.

To test this, we first confirmed that cysteine binds to silicate surfaces through its sulfur and carboxylate groups simultaneously. Amino acid surface attachment results in changes in its electronic environment, which can be observed in NMR spectroscopy. Solid state ^{13}C cross

polarization spectra of silicate/cysteine complexes revealed multiple resolvable signals attributable to silicate-bound cysteine (**Figure 3a**), which exhibited chemical shifts distinct from that of unbound cysteine or cystine (**Figure S6**). For L-cysteine, three $^{13}C_\beta$ resonances with similar or identical chemical shifts were resolvable in samples prepared at both pH 1.5 and pH 10.5 (**Figure 3b**), indicating that the sulfur attachment occurs over a wide pH range. The two upfield shifted $^{13}C_\beta$ signals likely indicated the presence of noncovalent, electrostatically bound complexes of the cysteine sulfur group with the silicate surface. In contrast, the downfield shifted $^{13}C_\beta$ signal at 43ppm agreed with the chemical shift reported for the $^{13}C_\beta$ of cysteine bound to gold (40), and likely reflects a covalent silicothioether bond (–Si-S-C(H_2)–). The presence of this covalent bond was confirmed by Polarization Resolved Infrared Reflection Absorption Spectroscopy (PR-IRRAS) (41) on samples of cysteine adsorbed to silicate films, which showed an absorption band for p polarized light at 1407cm^{-1} (**Figure S7**), consistent with the previously reported IR absorption of the Si-S-CH_2 in silicon bound ethanethiol (1406cm^{-1}) (42).

In contrast to the $^{13}C_\beta$ signals, the $^{13}C_\alpha$ of L-cysteine exhibited a single resonance in all samples but with stereospecific chemical shifts and line-broadening (**Figure 3**). At pH 10.5, the $^{13}C_\alpha$ chemical shift (51.58ppm) was shifted upfield relative to the silicate-free cysteine $^{13}C_\alpha$ (54.69ppm), consistent with a significant electronic change attributed to bivalent binding to silicate. The pH 1.5 chemical shifts of the L-cysteine $^{13}C_\alpha$ and carboxylate ^{13}C were consistent with monovalent association and the release of the carboxylate/silicate interaction: the cysteine $^{13}C_\alpha$ chemical shift at low pH (54.65ppm) was similar to that of silicate-free cysteine (54.69ppm), and the intense, upfield shifted carboxylate ^{13}C resonance observed at pH 10.5 (170.82 and 167.02ppm) was replaced at pH 1.5 by two downfield shifted carboxylate resonances (172.37ppm and 170.54ppm). Given that the cysteine carboxylate has a pK_a of 1.92, we attributed the signal at 172.37ppm to the protonated carboxylate, similar to that of the free cysteine (172.11ppm), and the signal at 170.54 was attributed to the deprotonated carboxylate.

The high pH NMR spectra of D-cysteine bound to silicate indicated a similar number of $^{13}C_\beta$ signals and with similar chemical shifts, consistent with sulfur-driven attachment, but with lower signal-to-noise. The D-cysteine $^{13}C_\alpha$ signal was notably shifted and broadened compared with that of L-cysteine (**Figure 3ac**), confirming that L- and D- enantiomers of cysteine have stereospecific physical properties when bound to mineral surfaces.

We conclude that cysteine attaches bivalently through both the sidechain sulfur and mainchain carboxylate at high pH but is attached predominantly monovalently via a sidechain sulfur at low pH. The association of cysteine with silicate via the thiol group at low pH demonstrates that the catalytic effect from increased residence time on the silicate surface would be applicable across a wide pH range. The stereoselectivity of this catalytic effect is expected to be possible at any pH greater than the pK_a of the cysteine carboxylate (>pH 2.0), to enable bivalent attachment, however detectable peptide synthesis yields are restricted to alkaline pH (>9.50), which is required for amino group deprotonation (14).

Stereospecific reorientation of the amino group in bivalently silicate adsorbed D-amino acids

The different physical properties that arise from bivalent surface attachment of enantiomers were investigated further by PR-IRRAS, which provides bond angle information for surface adsorbed molecules. We predicted that a stereospecific reorientation of the amino group, which is the site of peptide bond formation, should be observed for amino acids capable of bivalent

surface attachment but not for amino acids restricted to monovalent attachment at alkaline pH. Following incubation with SiO_2, all samples including the L- and D-alanine controls showed reflectance in p polarized light but not s polarized light, consistent with the signals arising from surface-bound amino acids. A clear stereospecific inversion of the reflectance corresponding to the amino group (N-H) asymmetric bend (43) was observed for bivalently bound cysteine and aspartate amino acids (**Figure 4a-b)** but not for the alanine control (**Figure 4c**). The amino group band inversion observed for bivalently silicate adsorbed D-amino acids indicates a different orientation of these amino groups relative to the plane of the surface compared to their L-enantiomers, and provides a likely mechanism for the observed stereoselective differences in the rate of peptide bond formation observed for cysteine.

Discussion

How and why life began to make exclusive use of L-amino acids from a racemic prebiotic amino acid mixture is an open question (18). We propose that the presence of cysteine within a surface-catalyzed peptide synthesis system modeled on alkaline hydrothermal vents could have a significant impact on peptide formation rates and could feasibly provide a stereoselective bias for prebiotic chemistry. Cysteine enriched peptides have the additional benefit of being capable of spontaneous metal ligation and redox activity (35, 36).

We show that the addition of cysteine to the conventional set of ten abiotically available amino acids significantly increases peptide yield when heated in the presence of an oxide-mineral in alkaline conditions. High peptide yields depended on the presence of a mineral substrate, indicating that peptide formation occurs predominantly through surface catalysis. We also show that cysteine interacts bivalently with silicate surfaces via a covalent Si-S bond and remains bound after multiple washes, in contrast to glycine, which adsorbs weakly to silicate surfaces and is almost completely removed after two wash cycles (44). Although the cysteine thiol interacts with silicates across a wide pH range, stereoselective and high peptide yields can only be achieved at alkaline pH because of the requirement for amino group deprotonation to achieve high peptide yields (14). The cysteine mineral attachment is reversible in peptides, as evidenced by the presence of readily purified cysteine bearing peptides in the supernatant.

Our peptide synthesis yields in the presence of cysteine displayed a marked stereoselective bias towards the L enantiomer, with a 50% increase in peptide yield when synthesis was conducted with L-cysteine compared to D-cysteine. The stereoselectivity of the yield was far greater than observed in previous salt-induced peptide synthesis experiments (27), and achieved in amorphous borosilicate glass. The increased yield in the presence of L-cysteine is attributed to the stereospecific orientation of the amino group when bivalently bound to a silicate surface. The amino group is the site of peptide bond formation, and its reorientation may change solvent accessibility or introduce steric clashes that affect surface residence times, which in turn affect the rate of peptide bond formation. We also found evidence of bivalent attachment of aspartate to silicate, and a corresponding stereospecific orientation of the aspartate amino group, but the much weaker nucleophilicity of the carboxylate and the corresponding weaker silicate association (38) precluded observation of a significant stereoselective effect for aspartate on the rate of peptide bond formation in our model system.

The presence of L-cysteine increased the lengths of peptides that were produced compared with either D-cysteine or L-alanine. Our ability to detect longer peptides is likely due in part to an overall increase in peptide yields, which suggests that cysteine incorporated into peptides retains an increased affinity for silicate surfaces.

Although the longest peptides observed with L-cysteine were higher than those detected here for L-alanine or reported elsewhere from oxide mineral catalyzed syntheses (22), these lengths are well below that of a typical modern, protein domain. Due to changes in charge density the strength of peptide binding to mineral surfaces decreases with increasing peptide length, which limits the concentration of longer peptides at the mineral surface. A combination of surface-catalyzed peptide elongation and peptide ligation in solution, facilitated by wet/dry cycles, has been proposed (45), but model systems restricted to meteoritic amino acids have provided only low yields of short peptides (22). The incorporation of cysteine into peptides opens the possibility for novel mechanisms of peptide elongation in solution catalyzed by metal ion binding via the sidechain thiol. Strong metal-sulfur binding would locally concentrate cysteine-bearing peptides, which may increase the probability of peptide ligation compared with the weaker metal chelation available to peptides restricted in composition to meteoritic amino acids.

Our results indicate that the cysteine thiol catalyzes efficient and stereoselective peptide synthesis in alkaline environments at 90˚C. Marine 'white smoker' hydrothermal vents found on Earth, and possibly also at the bottom of the Enceladian ocean (21), present suitable environments for such surface-catalyzed peptide synthesis reactions. Our results indicate that abiotic peptides synthesized in such environments are likely to be enriched with the L-enantiomer of cysteine, and possibly also L-aspartate(38), through stereospecific orientation of amino groups that results from bivalent surface attachment. Such disproportionate incorporation of a subset of L-amino acids may have provided the stereochemical bias leading to L-amino acid homochirality through stereospecific amplification (26, 46, 47).

The presence of an amino acid with a highly nucleophilic thiol would confer major benefits to early life including high yield and stereoselective peptide synthesis that results in peptides capable of forming metal complexes and feasibly participate in early metabolism. For example, cysteines can bind and stabilize redox-active FeS clusters (33), which are present in some of the most ancient proteins (48). Considering the exceptional benefits of the thiol group, it is intriguing to note that all modern proteins begin with a sulfur-bearing methionine. Our findings provide further motivation for investigating the availability of cysteine or related thiol-containing amino acids on early Earth and whether the presence of such molecules could be a practically useful biosignature for life elsewhere.

References

1. Farías-Rico JA & Mourra-Díaz CM (2022) A short tale of the origin of proteins and ribosome evolution. *Microorganisms* 10(11): 2115.

2. Pizzarello S & Shock E (2010) The organic composition of carbonaceous meteorites: The evolutionary story ahead of biochemistry. *Cold Spring Harb Perspect Biol* 2(3): a002105.

3. Oba Y, *et al* (2022) Identifying the wide diversity of extraterrestrial purine and pyrimidine nucleobases in carbonaceous meteorites. *Nat Commun* 13(1): 1–10.

4. Fried SD, Fujishima K, Makarov M, Cherepashuk I & Hlouchova K (2022) Peptides before and during the nucleotide world: An origins story emphasizing cooperation between proteins and nucleic acids. *J R Soc Interface* 19(187): 20210641.

5. Higgs PG & Pudritz RE (2009) A thermodynamic basis for prebiotic amino acid synthesis and the nature of the first genetic code. *Astrobiology* 9(5): 483–490.

6. Zaia DAM, Zaia CTBV & De Santana H (2008) Which amino acids should be used in prebiotic chemistry studies?. *Orig Life Evol Biosph* 38(6): 469–488.

7. Brotzel F & Mayr H (2007) Nucleophilicities of amino acids and peptides. *Org Biomol Chem* 5(23): 3814–3820.

8. Fitz D, Jakschitz T & Rode BM (2011) in *Origins of Life: The Primal Self-Organization,* eds Egel R, Lankenau D & Mulkidjanian AY (Springer Berlin Heidelberg, Berlin, Heidelberg), pp 109–127.

9. Wang W, *et al* (2021) Water microdroplets allow spontaneously abiotic production of peptides. *J Phys Chem Lett* 12(24): 5774–5780.

10. Sumie Y, Sato K, Kakegawa T & Furukawa Y (2023) Boron-assisted abiotic polypeptide synthesis. *Commun Chem* 6: 89.

11. Bernal JD (1949) *The physical basis of life. Science* 115(2976): 50.

12. Lambert J (2008) Adsorption and polymerization of amino acids on mineral surfaces: A review. *Orig Life Evol Biosph* 38(3): 211–242.

13. Kitadai N, *et al* (2017) Glycine polymerization on oxide minerals. *Origins of Life and Evolution of Biospheres* 47(2): 123–143.

14. Rodriguez-Garcia M, *et al* (2015) Formation of oligopeptides in high yield under simple programmable conditions. *Nature Communications* 6(1): 8385.

15. Shock EL (1992) Stability of peptides in high-temperature aqueous solutions. *Geochimica Et Cosmochimica Acta* 56(9): 3481–3491.

16. Flegmann AW & Tattersall R (1979) Energetics of peptide bond formation at elevated temperatures. *J Mol Evol* 12(4): 349–355.

17. Takahagi W, *et al* (2019) Peptide synthesis under the alkaline hydrothermal conditions on enceladus. *ACS Earth Space Chem* 3(11): 2559–2568.

18. Kitadai N & Maruyama S (2018) Origins of building blocks of life: A review. *Geoscience Frontiers* 9(4): 1117–1153.

19. Waite JH, *et al* (2017) Cassini finds molecular hydrogen in the enceladus plume: Evidence for hydrothermal processes. *Science* 356(6334): 155–159.

20. Glein CR & Waite JH (2020) The carbonate geochemistry of enceladus' ocean. *Geophys Res Lett* 47(3): e2019GL085885.

21. Choblet G, *et al* (2017) Powering prolonged hydrothermal activity inside enceladus. *Nature Astronomy* 1(12): 841–847.

22. Cleaves HJ, Aubrey AD & Bada JL (2009) An evaluation of the critical parameters for abiotic peptide synthesis in submarine hydrothermal systems. *Origins of Life and Evolution of Biospheres* 39(2): 109–126.

23. Lemke KH, Rosenbauer RJ & Bird DK (2009) Peptide synthesis in early earth hydrothermal systems. *Astrobiology* 9(2): 141–146.

24. Robinson KJ, *et al* (2021) Quantifying the extent of amide and peptide bond synthesis across conditions relevant to geologic and planetary environments. *Geochim Cosmochim Acta* 300: 318–332.

25. Otake T, *et al* (2011) Stability of amino acids and their oligomerization under high-pressure conditions: Implications for prebiotic chemistry. *Astrobiology* 11(8): 799–813.

26. Chen Y & Ma W (2020) The origin of biological homochirality along with the origin of life. *PLOS Computational Biology* 16(1): e1007592.

27. Plankensteiner K, *et al* (2004) Indications towards a stereoselectivity of the salt-induced peptide formation reaction. *Inorganica Chimica Acta* 357(3): 649–656.

28. Hazen RM, Filley TR & Goodfriend GA (2001) Selective adsorption of l- and d-amino acids on calcite: Implications for biochemical homochirality. *Proceedings of the National Academy of Sciences* 98(10): 5487–5490.

29. Rout SK, Rhyner D, Riek R & Greenwald J (2022) Prebiotically plausible autocatalytic peptide amyloids. *Chem Eur J* 28(3): e202103841.

30. Goldford JE, Hartman H, Marsland R & Segrè D (2019) Environmental boundary conditions for the origin of life converge to an organo-sulfur metabolism. *Nature Ecology & Evolution* 3(12): 1715–1724.

31. Foden F, *et al* (2020) Prebiotic synthesis of cysteine peptides that catalyze peptide ligation in neutral water. *Science* 370(6518): 865–869.

32. Deng M, Yu J & Blackmond DG (2024) Symmetry breaking and chiral amplification in prebiotic ligation reactions. *Nature* 626(8001): 1019–1024.

33. Jordan SF, *et al* (2021) Spontaneous assembly of redox-active iron-sulfur clusters at low concentrations of cysteine. *Nat Commun* 12(1): 1–14.

34. Lee S, Kim SM & Lee RT (2013) Thioredoxin and thioredoxin target proteins: From molecular mechanisms to functional significance. *Antioxid Redox Signal* 18(10): 1165–1207.

35. Lukács M, Csilla Pálinkás D, Szunyog G & Várnagy K (2021) Metal binding ability of small peptides containing cysteine residues. *ChemistryOpen* 10(4): 451–463.

36. Bonfio C*, et al* (2017) UV-light-driven prebiotic synthesis of iron–sulfur clusters. *Nature Chem* 9(12): 1229–1234.

37. Goldfarb AR, Saidel LJ & Mosovich E (1951) The ultraviolet absorption spectra of proteins. *J Biol Chem* 193(1): 397–404.

38. Erastova V, Degiacomi MT, Fraser D,G. & Greenwell HC (2017) Mineral surface chemistry control for origin of prebiotic peptides. *Nat Commun* 8(1): 1–9.

39. Cottrell TL (1958) The strengths of chemical bonds

40. Abraham A, Mihaliuk E, Kumar B, Legleiter J & Gullion T (2010) Solid-state NMR study of cysteine on gold nanoparticles. *J Phys Chem C* 114(42): 18109–18114.

41. Flach CR, Gericke A & Mendelsohn R (1997) Quantitative determination of molecular chain tilt angles in monolayer films at the air/water interface: Infrared reflection/absorption spectroscopy of behenic acid methyl ester. *J Phys Chem B* 101(1): 58–65.

42. Blyholder G & Bowen DO (1962) Infrared spectra of sulfur compounds adsorbed on silica supported nickel . *J Phys Chem* 66(7): 1288–1292.

43. Barth A (2000) The infrared absorption of amino acid side chains. *Prog Biophys Mol Biol* 74(3): 141–173.

44. Lopes I, Piao L, Stievano L & Lambert J (2009) Adsorption of amino acids on oxide supports: A solid-state NMR study of glycine adsorption on silica and alumina. *J Phys Chem C* 113(42): 18163–18172.

45. Rode BM, Son HL & Suwannachot Y (1999) The combination of salt induced peptide formation reaction and clay catalysis: A way to higher peptides under primitive earth conditions. *Orig Life Evol Biosph* 29(3): 273–286.

46. Blackmond DG (2010) The origin of biological homochirality. *Cold Spring Harb Perspect Biol* 2(5): a002147.

47. Gleiser M & Walker SI (2012) Life's chirality from prebiotic environments. *International Journal of Astrobiology* 11(4): 287–296.

48. Alva V, Söding J & Lupas AN (2015) A vocabulary of ancient peptides at the origin of folded proteins. *eLife* 4: e09410.

Methods

Peptide Synthesis Reactions

Scourie Mòr pyroxenite was crushed and mesh filtered to less than 106µm. 50g of the resulting powder was cleaned by washing and drying at 120°C for 2 hours with 2x 50ml 60% ethanol (Diluted from 100% Stock (Ethanol Absolute VWR chemicals) and 2x 50ml MilliQ H_2O across four heat-drying cycles. After cleaning the pyroxenite was heated for a further 24 hours at 200°C. 0.06g/ml (of reactant) of cleaned sterilized Scourie Mòr pyroxenite was added into to 100ml borosilicate crimp neck vials (VWR, 548-0609) (50ml experiments) or 15ml polypropylene screw cap tubes (SARSTEDT, 62.554.502) (5ml experiments) to simulate a mineral/ocean interface near a hydrothermal system. For experiments using different oxide minerals, spectroscopy pure SiO_2, AlO_2, MgO_2 and FeO_2 was added to each reaction vessel as supplied (Sigma-Aldrich).

20mM total L- or L+D (1:1) MAAM solutions were prepared from crystalline powders as supplied (>98%, Thermo Fisher Scientific) in the following proportions: glycine (0.41), alanine (0.24), aspartate (0.12), glutamate (0.10), valine (0.04), serine (0.02), isoleucine (0.02), leucine (0.01), proline (0.03), and threonine (0.01). For experiments using isotopically labelled amino acids, crystalline L-cysteine (99% 3-^{13}C, Cambridge Isotope Laboratories), glycine ^{15}N (98% ^{15}N, Sigma-Aldrich), L-methionine ($^{13}C_{methyl}$) (Sigma-Aldrich) and L-alanine ^{15}N (98% ^{15}N, Cambridge Isotope Laboratories) were used. The amino acid mixtures were dissolved in 0.1M bicarbonate/carbonate buffer (pH 9.55±0.1) that had been prepared from anhydrous sodium carbonate (Fisher Scientific) and sodium bicarbonate (ACS grade, Sigma). Once all amino acids were fully dissolved, 500mM NH_4OH was added from a 28-30% NH_4OH stock solution (ACS grade, 28-30% in water, Thermo Fisher Scientific) and the pH adjusted with 33% HCl or 5M NaOH to 9.55±0.1.

20mM stocks of each 'excess' amino acid to be tested (>98%, Thermo Fisher Scientific) were prepared separately in 0.1M bicarbonate/carbonate buffer (pH 9.55±0.1). Solutions contained 20mM Na_2S (ACS grade, MP Biomedical) or 20mM TCEP (Fluorochem) prior to mixing to prevent amino acid oxidation before or after peptide synthesis. The measured redox potential was typically 90-100mV following synthesis. All solutions were sparged for 20 minutes in N_2 followed by a further 30-minute equilibration in a 100% N_2 atmosphere (<10 O_2 ppm) in a positive pressure anaerobic hood (COY Laboratory Products).

Following N_2 equilibration, the MAAM solutions and the excess amino acid solution were added to the borosilicate or polypropylene reaction vessel with 0.06g/ml pyroxene or other oxide mineral. The solutions were diluted with 0.1M carbonate buffer (pH 9.55±0.1) to a final concentration of 5mM MAAM, 5mM TCEP or Na_2S, 250mM NH_4OH, and 5mM of the excess amino acid. The reaction vessels were crimp sealed or screw capped and heated at 90°C (Heratherm OGS100).

At reaction completion, the reaction vessels were removed from the oven and uncapped within a fume hood while cooling to room temperature. Solutions were vacuum pump filtered through a 0.22µm polyethersulfone (PES) membrane (MilliPore). The resulting amino acid/peptide mixtures were stored at -80°C until analyzed by UV-spectrophotometry or lyophilized in 20 or 1ml aliquots.

C18 Peptide Purification

Post-reaction samples for TIMS-TOF MS were purified by C18 chromatography prior to loading. 4ml aliquots of post-reaction sample were lyophilized and resuspended into 400µl of 0.1% trifluoracetic acid (TFA) (Sigma-Aldrich). Separately, C18 SPE tips were prepared by packing 2µl of C18 resin (Empore SPE C18 48mm 12um particle size) into 10µl micropipette tips. The resin was activated by washing twice with 60µl of 100% acetonitrile (HPLC grade, 99.9%, Sigma-Aldrich) and 60µl of 0.1% TFA (Sigma-Aldrich) with a 2-minute spin at 4000x*g* after each addition. 400µl of sample in 80µl aliquots was then pipetted into each SPE tip with a 4-minute spin at 5000x*g* after each addition. The flowthrough was retained, and the column washed with 60µl of 0.1% TFA. Peptides were eluted in 160µl of 60% acetonitrile in 80µl aliquots. Elution fractions were lyophilized and stored at 4°C prior to analysis.

UV-Vis Spectrophotometry

Post-reaction samples in 0.1M carbonate at pH 9.5 were diluted 1 in 20 with 0.1M carbonate buffer at pH 9.5 (prepared as described above) to 200µl. 200µl of the diluted aliquots were added to an HellmaAnalytics High Precision Quartz SUPRASIL UV-Vis cell (light path 10x2mm) and were scanned at wavelengths of 200-800nm in a Cary 50 Bio UV-Visible Spectrophotometer with a scan rate of 4800.000nm/min and 1.0nm data intervals in dual beam mode with a baseline correction against a 0.1M carbonate pH 9.5 solution. Three technical repeats were recorded for each sample and the mean reported as a single biological repeat for comparison between synthesis runs. The UV-Vis cell was cleaned between samples with 1ml of 2% Hellmanex III (Sigma Aldrich) and thoroughly rinsed with Milli-Q water between each experiment and dried with N_2 gas. Biological repeats were normalized relative to L-alanine. Results were exported with the absorbance at 230.04nm plotted for each experiment using GraphPad Prism Software. For measurement of rates of apparent peptide bond formation, concentrations were estimated using 10mM dialanine (A_{230} = 0.45) as an internal calibration standard.

Statistical Analysis of UV-Vis Results

The statistical significance of results acquired by UV-Vis was determined by 1 way ANOVA with Tukey Post Hoc analysis of the mean absorbance values (2-3 technical repeats per sample) of post-reactive solutions following heating as reported for Figure 1a. An unpaired two tailed T test was used instead for data reported in Figure 1b.

TIMS-TOF MS

TIMS-TOF MS was conducted on purified peptide solutions following C18 SPE purification (described above). 1µl of purified peptides in 0.1% FA was injected onto a Bruker nanoElute HPLC equipped with a ThermoTrap Cartridge Guard Column (Thermo Scientific 160454) and a Bruker PepSep Fifteen elution column operating at 50°C (Bruker, 1893473). Peptides were eluted on to a Bruker timsTOF Pro 2 Mass spectrometer by gradient elution at a flow rate of 0.55ul/min (Buffer A - 0.1% FA, Buffer B – 100%ACN 0.1% FA) on a 30 minute 0-40% ACN gradient). Detections were analyzed within the Bruker Direct Analysis software. Peak lists were analyzed using a python script (written in house, and available on request) which compared exported mass detections to a list of every amino acid combination of peptides up to 20 amino acids long, and candidate peptides with >5ppm deviation in mass were discarded. For detections where multiple sequence combinations were possible, the identification with the

lowest ppm error with the detected mass was retained. Detections identified also in the negative control were removed. Detections with elution times less than 18 minutes (≈20% ACN) or greater than 28.5 minutes (≈38% ACN), and those with signal-to-noise ratios <2, were also removed.

Solution State Nuclear Magnetic Resonance (NMR)

Lyophilized crude or C18 SPE purified post-reaction solutions (1mL original volume) were resuspended into 200µl of water with 5% D_2O and 0.4mM DSS (Cambridge Isotope Laboratories) at pH 5.5 or in 99.9% D_2O (Sigma-Aldrich) with 5mM benzoic acid (ACS grade 99.5%, Thermo Fisher Scientific) and 0.4mM DSS (Cambridge Isotope Laboratories) at pH 5.5. The resulting 5x concentration solutions were loaded into 3mm Bruker SampleJet NMR tubes. NMR data were recorded in magnets operating at 17.6 or 22.3 Tesla (Oxford Instruments magnets) and equipped with high sensitivity 5mm TCI cryoprobes and Avance III HD consoles (Bruker). 2D ^{1}H,^{13}C heteronuclear single quantum correlation (HSQC) spectra were acquired with 64 scans, and the total points and sweep widths were 1274 and 320, and 11.934ppm and 65.00ppm, for ^{1}H and ^{13}C, respectively. 2D total correlation spectroscopy (TOCSY) data were acquired with 128 scans, sweep widths of 10.000ppm, and total points of 2048 and 320 in the direct and indirect ^{1}H dimensions, respectively. qNMR to measure depletion of monomeric amino acids was performed by integrating and comparing the $^{1}H\alpha$ signals from monomeric amino acids before and after reaction. The integrated triplet signal of benzoic acid centered at 7.403ppm at 20˚C was used as an internal standard to enable quantitative comparison between experimental runs. The results were analyzed with TopSpin 4.3.0.

Preparation of SiO_2/amino acid complexes

SiO_2/amino acid complexes were prepared using the approach of Lopes et al.(44) Solid amino acid/SiO_2 samples were prepared in a 100% N_2 gas atmosphere (<10ppm O_2) to eliminate the requirement for reducing agents during the mixing stage. 500mM solutions of L- or D-cysteine were prepared by dissolution of crystalline cysteine (>99%; Thermo Fisher Scientific) in Milli-Q water, the pH was adjusted to 1.5 or 10.5 using 33% HCl or 5M NaOH. For each reaction, 3.0g of SiO_2 (Specpure, Alfa Aesar) was weighed out and placed into a 50ml polypropylene tube (Sarstedt). Amino acid solutions were added to the SiO_2 powder and the tubes screwed-capped. The samples were stirred with a magnetic stir bar for 48 hours at 23°C.

Following mixing, the solutions were vacuum pump filtered through a 0.22µm PES membrane (MilliPore) to remove free amino acids. The SiO_2 solid left on the disk was gently washed and filtered three times with 30ml of 0.1M carbonate at pH 10.5 or pH 1.5. Following washing, the SiO_2 solid was scraped from the membrane and put into a 50ml polypropylene tube and lyophilized prior to storage at -80°C before analysis.

^{13}C Solid State NMR

Solid SiO_2/cysteine complexes, and control powders of free cysteine (99%, Thermo Fisher Scientific) and cystine (99%, Thermo Fisher Scientific) were loaded into a 100µl rotor. Solid state NMR data were recorded at 9.4 Tesla magnet equipped with an Avance III console (Bruker). ^{13}C cross polarization experiments were recorded with 4096 points and a sweep width of 405 ppm. Data on post-reaction samples were recorded with 80000-100000 scans, whereas data for the L-cysteine and L-cystine controls were recorded with 64 scans. NMR data was analyzed with TopSpin 4.3.0.

PR-IRRAS sample production and data collection

$Ti/Au/SiO_2$ microfilm slides mounted on a standard glass slide were prepared at the Thin Film Facility in the Department of Physics, University of Oxford. Glass microscope slides were cleaned prior to coating with Decon 90 and rinsed with deionized water, acetone and IPA. Slides were loaded into a Leybold L560 and cleaned by Argon glow discharge for 10 minutes ($6x10^{-2}$ mbar). Ti was evaporated using an e-beam ($4x10^{-5}$ mbar) and deposited at a rate of 0.3nm/s to a final thickness of 2nm. Au was evaporated by thermal evaporation at ($2x10^{-5}$ mbar) and deposited at a rate of 0.5nm/s to 10nm thickness. Finally, SiO_2 was evaporated using an ebeam ($2.2x10^{-5}$ mbar) and deposited at a rate of 0.25nm/s to a thickness of 10nm. Following preparation, the slides were moved to an anaerobic hood and placed at the base of a polypropylene container. Separately, 25mM solutions of D- and L-aspartate and solutions of 50mM D- and L-cysteine and D-and L-alanine were made up in Milli-Q water under a 100% N_2 atmosphere. Solution pH was adjusted to 10.0 using 5M NaOH and each added to a container with a $Ti/Au/SiO_2$ slide. The set up was incubated for 36 hours at room temperature. Following incubation, the slides were removed and washed using 20ml of pH 10.00 degassed Milli-Q water before being dried at room temperature prior to analysis. PR-IRRAS spectra for the $Ti/Au/SiO_2$ amino acid complexes were recorded on a Bruker Vertex 80 FT-IR spectrometer equipped with a liquid N_2 cooled MCT detector and a Pike VeeMax accessory. The spectrometer was referenced to a blank $Ti/Au/SiO_2$ slide, and the samples were assessed with s-polarized and p polarized beams at incidence angles of 30˚, 60˚ and 80˚. Absolute reflectance of p polarized beams was plotted using GraphPad Prism software.

Additional Information

Author Contributions

DPM, JW and JRS, conceptualized and designed the research, DPM performed data acquisition and analysis alongside IBR, and the results were interpreted by DPM, JRS and JW. The manuscript was prepared jointly by DPM, IBR, JW and JRS.

Competing Interest Statement

The authors declare no competing interests.

Data Sharing Plans

All data supporting the results of this paper have been retained and are available upon reasonable request.

Funding Information

This research was funded by the European Space Agency (4000136840) (DPM), the International Space School Education Trust (DPM), and the Department of Biochemistry (DPM, JRS), and St. John's College (JRS).

Acknowledgements

We acknowledge the following for their contributions: Professor Christina Redfield and the Biochemistry solution state NMR Facility, Dr. Julie Cosmidis (Department of Earth Sciences) for use of anaerobic hood facilities, Dr. Robert Jacobs (Department of Chemistry) and the Surface Analysis Facility for us of their PR-IRRAS and Infrared instruments, Dr. Nick Rees and the Solid State NMR Facility (Department of Chemistry) for use of their 400MHz solid state NMR instrument, the Thin Film Facility (Department of Physics) for provision of the Titanium/Gold/SiO_2 thin films, and Dr. Rod Chalk and the Centre for Medicine Discovery for use of their Mass Spectrometry Facility. We thank Dr Clinton Lau, Dr Harry McClelland and Dr Robert Lindner for discussions and comments on the manuscript.

Figures

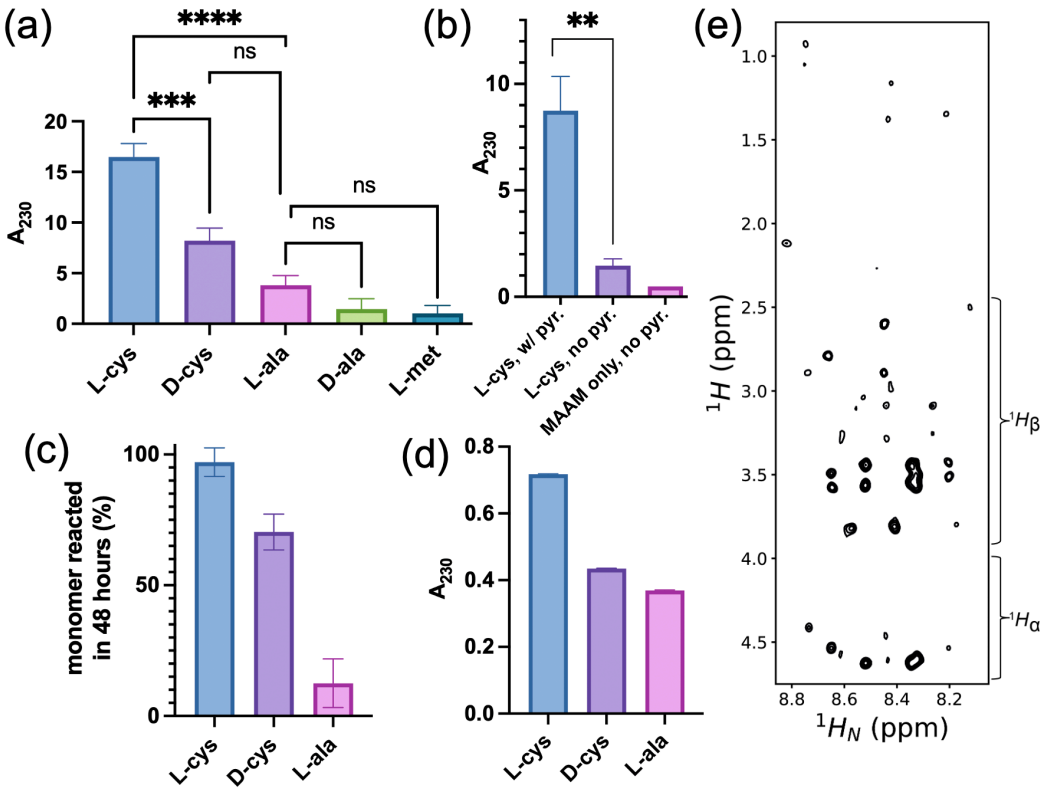

Figure 1: Cysteine stereo-specifically increases peptide yield in the presence of an achiral oxide mineral. *(**a**) Detection of peptide bond formation by absorbance at 230nm (A_{230}) after 48 hours of heating in borosilicate reaction vessels with MAAM plus an excess of L-cysteine (n=6), D-cysteine (n=5), L-alanine (n=6), D-alanine (n=3), or L-methionine (n=2). Biological repeats were normalised to the A_{230} with L-alanine. Normalisation relative to L-cysteine was used to determine the standard error of the mean (SEM; error bars) of L-alanine biological repeats. The mean control absorbance of L-alanine, D-alanine and L-methionine was 2.10. Significance was determined by one way ANOVA with Tukey post-hoc analysis of absorbance vs L-alanine (L-cysteine, p=<0.0001; D-cysteine, p=0.085; D-alanine, p=0.712; L-methionine, p=0.702) (**Table S1**). (**b**) A_{230} amino acid mixtures reacted in polypropylene reaction vessels with 5 mM L-cysteine, 5 mM MAAM and 0.5g pyroxene (L-cys, w/ pyr.; n=3), 5mM L-cysteine, 5mM MAAM, and no pyroxene (L-cys, no pyr.; n=3), and 10 mM MAAM with no L-cysteine or pyroxene (MAAM only, no pyr.; n=1). For the comparison of reactions containing L-cysteine and with or without pyroxene, p=0.0015 (two-tailed unpaired t-test) (**Table S2**). Error bars indicate SEM. (**c**) Loss of monomeric amino acid reactant by Quantitative NMR with a benzoic acid internal standard after 48 hours of reaction time. Error bars display standard deviation of the benzoic acid signal height at 7.4034ppm. (**d**) A_{230} measurement of stereoselective peptide bond formation following reactions at lower (55µM) amino acid starting concentrations. Reactions were heated at 90˚C for 42 days in borosilicate reaction vessels. Error bars indicate the standard deviation for technical repeats (n=3). (**e**) 2D ^{1}H-^{1}H TOCSY spectrum of a post-reaction mixture enriched in L-cysteine. The spectral region corresponds to intra-residue correlations between amide protons (^{1}HN) and either $^{1}H\alpha$ (~4.0 – 4.7ppm) or sidechain protons (~1.0 – 4.0 ppm).*

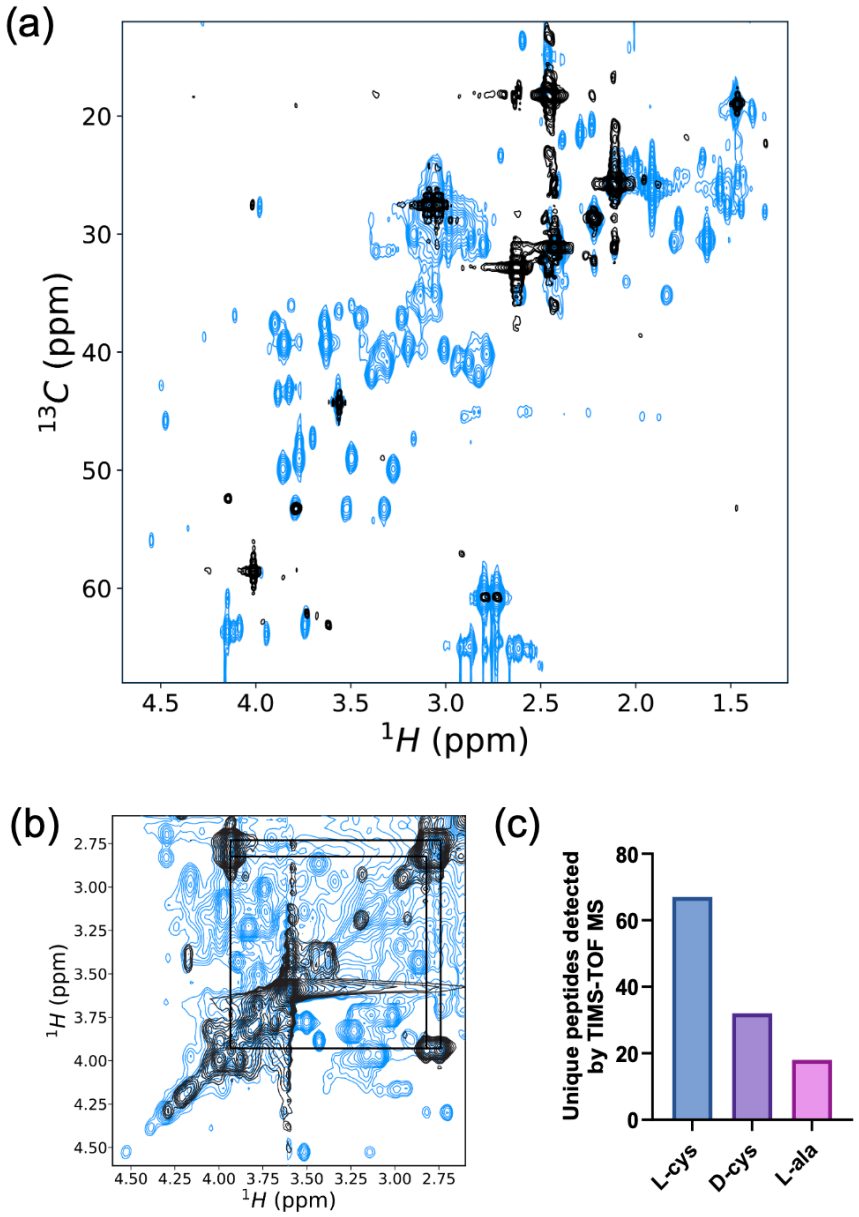

Figure 2: Peptide synthesis with cysteine yields a diverse set of cysteine-containing peptides. (a) Overlay of 2D ^{1}H-^{13}C HSQC spectra of reactions containing $^{13}C_{\beta}$-labelled L-cysteine before (black) and after (blue) reaction. New crosspeaks in the post-reaction spectrum are attributed to incorporation of $^{13}C_{\beta}$-labelled L-cysteine into peptides adjacent to different amino acid types. Additional crosspeaks arise from natural abundance ^{13}C (1.1%). **(b)** Overlay of 2D ^{1}H-^{1}H TOCSY spectra of reaction mixtures containing L-cysteine before (black) and after (orange) reaction. The intense cysteine monomer $^{1}H_{\alpha}$-$^{1}H_{\beta}$ crosspeaks observed before reaction are indicated by lines. The large number of new post-reaction crosspeaks are attributed to unique peptide species. **(c)** Histogram of the total number of unique peptide products in L-cysteine reactions identified by TIMS-TOF MS after purification by SPE and HPLC prior to MS loading.

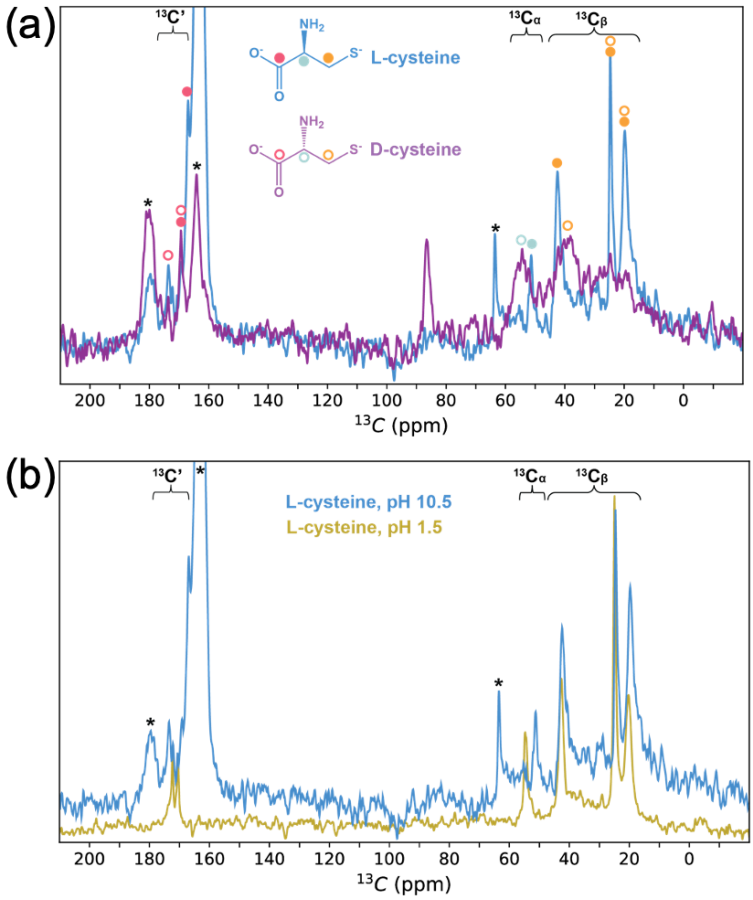

(c)

	^{13}Cα (*ppm*)	^{13}Cβ (*ppm*)			^{13}COOH (*ppm*)	
L-cysteine, free	54.69	26.81			172.11	
L-cystine, free	52.36	34.01			173.74	
L-cysteine, bound, pH 1.5, monovalent	54.65	42.76	24.91	20.26	172.37	170.54
L-cysteine, bound, pH 10.5, bivalent	51.58	42.74	24.95	20.37	170.82	167.02
D-cysteine, bound, pH 10.5, bivalent	*60.3-51.2 (broad)*	*45.1-37.8 (broad)*	*26.9-24.1 (broad)*	*23.4-17.3 (broad)*	*171.28*	

Figure 3: D-cysteine and L-cysteine association with silicates is bivalent at alkaline pH. (a) Overlay of solid-state NMR ^{13}C cross polarisation spectra of L-cysteine (blue) and D-cysteine (purple) absorbed to silicate at pH 10.5. The ^{13}C resonances are indicated by colored circles for L-cysteine (closed) and D-cysteine (open). Chemical shift positions of the enantiomers are similar for carboxylate ^{13}C' signals and differ for the ^{13}Cα and ^{13}Cβ signals. Wash buffer signals at 163.2ppm (bicarbonate), 169.3ppm (carbonate) 179.7ppm (carbonate salt), and 63.7ppm (bicarbonate sideband) are indicated (*). **(b)** Solid-state NMR ^{13}C cross polarisation spectra of L-cysteine absorbed to silicates at pH 10.5 (blue) and pH 1.5 (yellow). The ^{13}Cβ signals are independent of pH, whereas the ^{13}Cα and carboxylate ^{13}C' signals are perturbed at low pH consistent with de/protonation of the carboxylate. (**c**) ^{13}C chemical shifts determined from solid-state spectra. Asterisks indicate the observed chemical shifts consistent with covalent thiolate attachment[42].

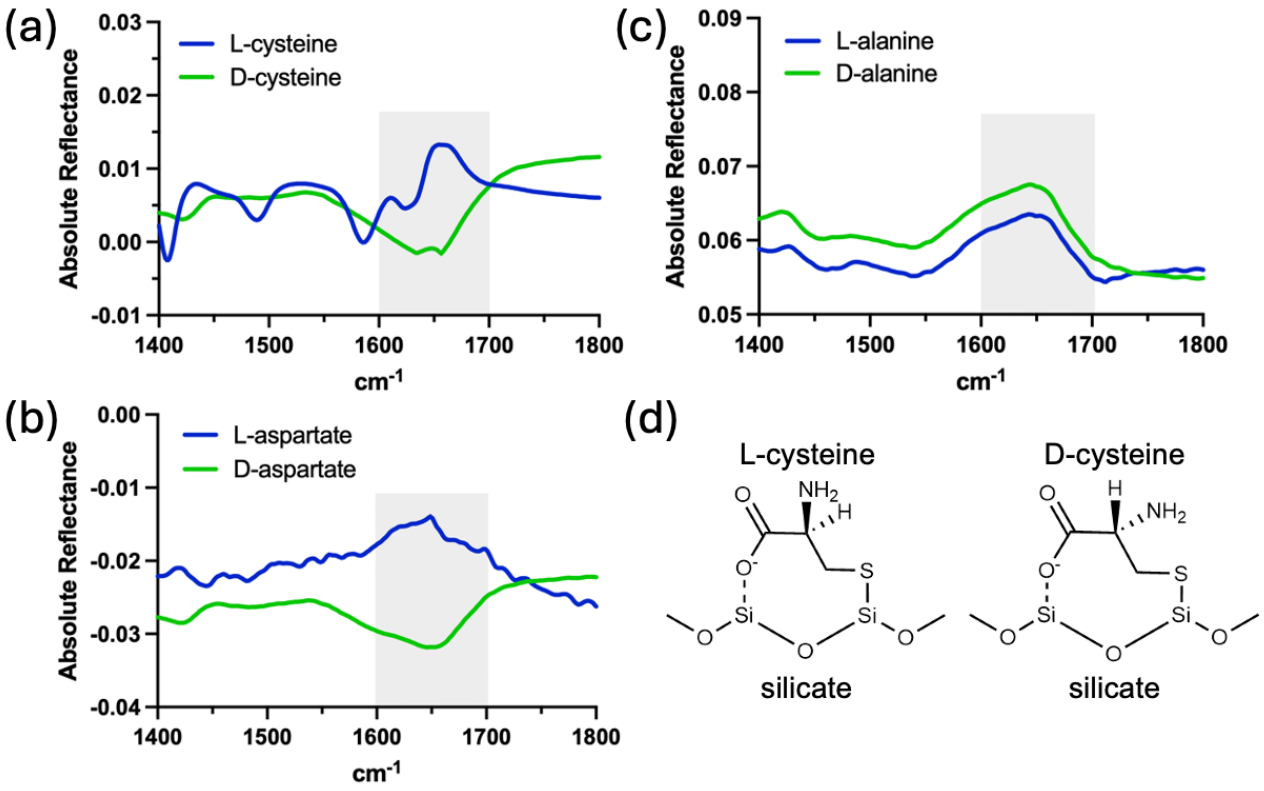

Figure 4: Bivalent surface attachment stereo-specifically orients the amino acid amino group. PR-IRRAS of the enantiomers of **(b)** cysteine, **(c)** aspartate, and **(d)** alanine absorbed to silicate. Stereospecific inversion is observed in the reflectance corresponding to the asymmetric bend of the amino group (~1600-1700 cm^{-1}) in samples containing cysteine and aspartate but not alanine. Full spectra are shown in **Figure S8**. **(d)** Schematic of bivalently attached L- and D-cysteine indicating the proposed stereospecific orientation of the amino group.